Large-scale impurity potential and nature of the main low-temperature luminescence line of pure n-InSb crystals

I. V. Kavetskaya, N. B. Kakhramanov, N. N. Sibel'din, and V. A. Tsvetkov

P. N. Lebedev Physical Institute of the Academy of Sciences of the USSR

The main luminescence line of pure n-type indium antimonide crystals
($N_D - N_A = (0.3–2) \cdot 10^{14}$ cm^{-3}) and the absorption spectra in the region of the main line were
studied at liquid-helium temperatures. It was ascertained that the main emission line is associated
with transitions of electrons from narrow donor levels into the valence band and the spectral
position and shape of this line are determined by large-scale fluctuations of the concentration of
charged impurities. It was found that the nonequilibrium charge carriers fill a volume whose
linear dimensions are much greater (by approximately two orders of magnitude) than the
ambipolar diffusion length of the carriers.

INTRODUCTION

Indium antimonide is a classical material for studying a wide range of the most diverse physical phenomena. The modern technology of preparation of this semiconductor compound makes it possible to grow structurally perfect single crystals with a low content of residual impurities. It is largely because of this that indium antimonide is the most appropriate material for investigating exciton effects in narrow-band semiconductors.

Since the exciton binding energy in indium antimonide is small (≈ 0.5 meV), exciton lines are usually observed in the reflection spectra[1,2] and absorption spectra[3-5] only in a magnetic field, which stabilizes the weakly bound states. Emission lines of bound[6-8] and free[9] diamagnetic excitons of a magnetic-field-stabilized electron-hole liquid (EHL)[1),6] have been observed in the luminescence spectra of quite pure samples placed in a magnetic field.

For a long time the reliability of the interpretation of the edge luminescence spectra of indium antimonide in the absence of a magnetic field, which had already been studied in great detail by the mid-1970s,[12-15] has never been questioned. However, after Kanskaya et al.[16] observed an exciton maximum at the absorption edge of the samples subjected to special heat treatment, and, thanks to this, were able to determine the band gap more accurately [$E_g = 236.8 \pm 0.2$ meV at $T = 2$ K (Ref. 16)], it was found that the main emission line of quite pure n-type samples, which was usually associated with direct interband transitions, lies entirely at energies less than the band gap width. At the present time there is no general agreement as to the nature of this line. In Refs. 8, 9, and 17 it is conjectured that the main line of the spectrum is due to radiative recombination of electrons and holes in free or bound excitons. At the same time, in Refs. 18–20 data confirming the previous viewpoint are presented and the long-wavelength shift of the line is explained by the narrowing of the forbidden band as a result of interparticle interactions in the electron-hole plasma and as a result of the tails of the density of states (though the analysis of the experimental data was based on an obsolete value of the undisturbed band gap of 235.5 meV). Similar considerations were stated in Ref. 7.

Discrepancies have also appeared in the interpretation of the emission line arising under intense pumping on the long-wavelength wing of the main line (B-line, in the notation adopted in Refs. 9 and 17). In Ref. 17 it was suggested that this line can be attributed to excitons, bound with deep acceptors, and in Ref. 20 it was interpreted as a stimulated emission line of an electron-hole plasma. Other possibilities have also been discussed.[9]

In this paper we investigate the main luminescence line of pure n-type indium antimonide crystals over a wide range of intensities of photoexcitation at temperatures of 2–4.2 K and the absorption spectra in the region of the main line, and the shapes of the emission and absorption spectra are analyzed theoretically and compared with one another.[2)] It is shown that the spectral position and shape of the main emission line are determined by large-scale fluctuations of the concentration of charged impurities; these fluctuations give rise to bending of the edges of the allowed bands. The observed radiation is then associated with transitions of electrons from shallow donor levels, lying below the "dips" of the conduction band, into the spatially separated "hills" of the valence band, which are potential wells for holes.[3)] The data obtained also show that the line appearing with high excitation intensities is a superluminescence line and arises as a result of the same electronic transitions as in the case of the main line.

At first glance it appears somewhat unexpected that the large-scale impurity potential plays the main role in the formation of the emission spectrum of even extremely well-purified samples of indium antimonide. As the experimental results and theoretical estimates presented below show, however, even in this case the rms fluctuation potential is quite high (much greater than one electronic Rydberg), and the energy of the main edge-luminescence line is primarily determined by the depth and spatial extent of the potential wells formed by fluctuations of the concentration of the charged impurities.

In order to avoid misunderstandings, we emphasize once again that here we are talking about the luminescence spectrum in the absence of a magnetic field. In a sufficiently strong field, under certain conditions emission lines of exciton-impurity complexes[6,7] ($H > 5–7$ kOe) and EHL ($H \gtrsim 20$ kOe; Ref. 6) appear superposed on the main emission line. The appearance and properties of these lines are

completely unrelated to the characteristics of the luminescence spectrum as a function of the magnetic field strength and the level of excitation in weaker fields.

EXPERIMENTAL PROCEDURE

For investigation of luminescence either a Nd^{3+} YAG laser with wavelength $\lambda = 1.06\ \mu m$ and maximum power P_{max} of about 3 W or a He–Ne laser with $\lambda = 3.39\ \mu m$ and $P_{max} \simeq 15$ mW was employed for quasistationary excitation of the samples. Both lasers operated in the cw mode. The excitation radiation was modulated with a frequency of 1 kHz with a mechanical interrupter. In order to reduce the overheating of the sample occurring under intense pumping the ratio of the pulse period to the length of the excitation pulse was varied from 2:1 for low excitation levels up to 10:1 for high excitation levels. The diameter of the exciting light beam on the sample was equal to ~ 0.3 mm. The excitation intensity was varied with the help of neutral light filters.

Recombination radiation was collected either from the surface of the sample illuminated with the laser (reflection geometry) or from the opposite surface of the sample (transmission geometry). The radiation was analyzed with an MDR-2 monochromator with a grating of 100 lines/mm and recorded with a liquid-nitrogen-cooled Ge:Au photoresistor.

When the transmission spectra were measured, radiation from a globar lamp was first passed through the same monochromator and then focused on the sample. The transmission spectra of samples with different thickness d are presented in Fig. 1. The spectra were replotted taking into account the frequency dependence of the intensity of the globar radiation. The absorption spectrum $\alpha(\omega)$ was calculated from the same curves with the help of the approximate formula

$$t = (1-R)^2 e^{-\alpha d} \qquad (1)$$

(t and R are the transmission and reflection coefficients, respectively) by two methods. First, for each selected value of $\hbar\omega$ the absorption coefficient was determined from the slope of the straight line $\ln(t)$ versus d. Second, along each transmission curve shown in Fig. 1 α was calculated from its value at the point $\hbar\omega = 234.5$ meV, obtained by the first method. The spread in the computed values of $\alpha(\omega)$ was equal to

10% on the average. The dashed line in Fig. 1 shows the absorption spectrum.

The experiments were performed on samples of pure n-type indium antimonide with electron density $n = (0.3-2) \cdot 10^{14}$ cm^{-3} and electron mobility $\mu_e = (6-7.5) \cdot 10^5$ cm^2/(v·s) (n and μ_e were measured at $T = 77$ K). After mechanical polishing the samples were etched in SR-4A polishing etchant. The typical dimensions of the samples were $5 \times 5 \times (0.1-1.0)$ mm^3. The samples were freely suspended in the helium volume of a cryostat and during the experiment they were placed directly in the liquid helium.

EXPERIMENTAL RESULTS

The main emission lines of two samples of n-InSb at a temperature of $T = 2$ K and with a low level of excitation ($P \approx 10$ mW with $\lambda = 3.39\ \mu m$) are presented in Fig. 2 (reflection geometry). First of all, it should be noted that the main luminescence lines of all samples studied lie entirely in the range of energies less than the width of the band gap (and less than the energy of the transition into the state of a free exciton); at the same time, the maxima of these lines (≈ 235.3 meV for all samples) are appreciably shifted into the short-wavelength side of the significantly less intense emission line corresponding to transitions of free electrons into the levels of shallow acceptors (~ 227 meV). Further, as one can see from Fig. 1, as the concentration n increases the emission line widens and its wings become flatter.

Figure 3 shows the luminescence spectra in the region of the main emission line of samples of different thickness in the transmission geometry with a low level of excitation. The spectra are normalized so that the long-wavelength wings of the lines coincide. In reality the line intensities differ much more than is shown in the figure, and they are approximately inversely proportional to the thickness of the samples. As one can see from the figure, as the thickness of the sample increases the short-wavelength part of the spectrum is cut off. This cut-off is associated with the reabsorption (self-absorption) of recombination radiation in the volume of the
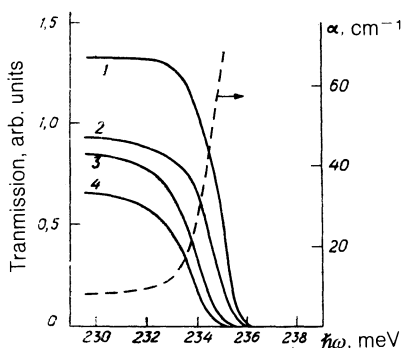

FIG. 1. Transmission spectra of samples of thickness $d = 100\ \mu m$ (1), 280 (2), 550 (3), and 850 (4). The difference of the impurity concentrations is $N_D - N_A \approx 1.2 \cdot 10^{14}$ cm^{-3} and the temperature is equal to 2 K. The dashed curve shows the spectral dependence of the absorption coefficient α (scale on the righthand side), calculated from the transmission spectra.
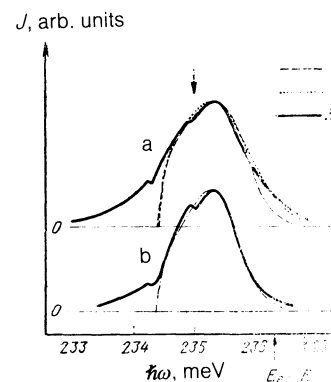

FIG. 2. The main luminescence lines of two samples with different differential concentrations of impurities $n = N_D - N_A$ in reflection geometry: a) $n \approx 1.2 \cdot 10^{14}$ cm^{-3}, b) $n \approx 3 \cdot 10^{13}$ cm^{-3}. The solid lines represent the experimental results and the curves 1–3 represent the calculations based on the formula (2) with $T = 2$ K (1, 3) and 3 K (2). The solid arrows mark the value of the width of band gap E_g and the energy of the transition into the ground state of a free exciton E_{ex} (according to Ref. 16). The dashed arrows show the position of the atmospheric water vapor absorption lines.
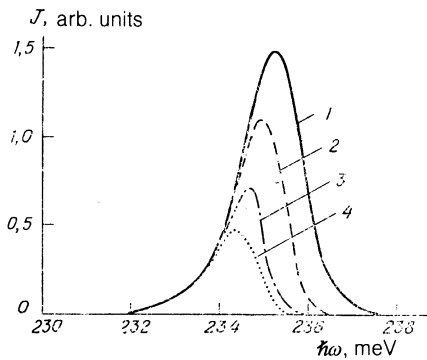
FIG. 3. Luminescence spectra of samples of different thickness d ($n \approx 1.2 \cdot 10^{14}$ cm^{-3} and the temperature is equal to 2 K) in transmission geometry ($P \approx 10$ mW with $\lambda = 1.06 \mu$m): $d = 100 \mu$m (1), 280 (2), 550 (3), and 850 (4).

sample.[15,22] In the reflection geometry the emission spectra of samples of different thickness had the same shape, practically identical to that of the spectrum of a sample of thickness $d \approx 100 \mu$m in the transmission geometry. Thus the self-absorption does not appreciably affect the shape of the main luminescence line in the reflection geometry. For this reason, in what follows, no correction is introduced for self-absorption in the theoretical analysis of the shape of this line.

For low levels of excitation ($\lesssim 10^{20}$ photons/cm$^2 \cdot$s) the shape and half-width of the main emission line were virtually independent of the pumping power, while the integrated intensity of this line increased quadratically as the excitation power increased. As the pumping intensity was increased further the growth of the integrated intensity of the emission line slowed down, but it remained superlinear in the entire range of excitation densities studied (the maximum excitation density was equal to $\approx 8 \cdot 10^{21}$ photons/cm$^2 \cdot$s).[4] For high levels of excitation the change occurring in the shape of the main luminescence line as the pumping power increases was found to be significantly different for thick (thickness $d \gtrsim 300 \mu$m) and thin samples. As the level of excitation increased the shape of the long-wavelength edge of the luminescence line of thick samples remained practically unchanged, while its short-wavelength wing became flatter, and it acquired a tail, extending to high energies, higher than the width of the band gap of the crystal (Fig. 4).

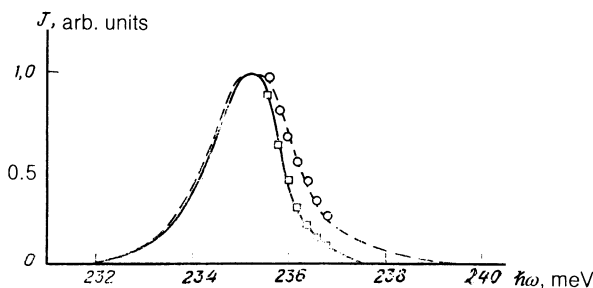As regards thin samples, the shape of the main lumines-

cence line was already appreciably distorted at moderate pumping intensities owing to intensification of recombination radiation in the volume of the sample, and under intense pumping a superluminescence line appeared on the long-wavelength wing of the main line. The results of the experiments with thin samples are not presented in this paper. For this reason, here we will not discuss this question further, and we merely note that in our opinion there are no grounds for associating the line (designated in Refs. 9 and 17 as the line B) arising under intense pumping with electronic transitions between some different states and not the same states which are responsible for the main spontaneous-luminescence line.

The experimental data presented above were obtained at a temperature of $T \approx 2$ K. At moderate pumping intensities an increase of the temperature of the helium bath up to $T \approx 4.2$ K did not lead to any appreciable change in the shape of the long-wavelength wing of the main emission line, while its short-wavelength edge was smeared to a greater or lesser degree (depending on the pumping intensity). At high pumping powers ($P \gtrsim 100$ mW) and $T = 4.2$ K the luminescence spectrum became strongly deformed owing to overheating of the sample even with the shortest ($\approx 100 \mu$s) excitation pulses. Since the experimental results obtained at $T = 4.2$ K do not contain any significant additional information, we shall confine ourselves to what we have said above and we shall not study these data in greater detail.

DISCUSSION

1. Preliminary remarks. As noted in the introduction, in most work the main recombination-radiation line was associated with direct interband transitions. This was done for the following reasons. The first one is that the value of the energy corresponding to the spectral position of the maximum of this line is close to the width of the band gap (more accurately, to its value $E_g \approx 235.7$ meV (Ref. 3) that was generally accepted prior to the appearance of Ref. 16).

The second reason is that the shape of the line is described quite well by the formula for direct allowed interband transitions:[15]

$$J(\hbar\omega) \propto \omega^2 (\hbar\omega - E_g)^{1/2} \exp\left[-\frac{m_e}{m_e + m_h} \frac{\hbar\omega - E_g}{kT} \right]$$

$$\times \left\{ \exp\left(\left[\frac{m_h}{m_e + m_h} (\hbar\omega - E_g) - E_F \right] \Big/ kT \right) + 1 \right\}^{-1}, \quad (2)$$

where E_F is the position of the Fermi quasilevel for electrons, m_e and m_h are the effective masses of the electrons and holes, respectively, and T is the temperature of the sample. This formula was obtained under the assumption that the nonequilibrium carriers in the bands are thermalized and that at low temperatures the electron distribution is degenerate while the hole distribution is described by Boltzmann statistics.

The results of the analysis of the shape of the main emission line of the two samples using the formula (2) are shown in Fig. 2. In the calculations the following values of the effective masses of the electrons and holes were employed: $m_e = 0.014 m_0$ and $m_h = 0.35 m_0$. The parameters E_g and E_F were adjusted so as to obtain the best agreement between the experimental and computational results. The experimental spectrum of the sample with $n \approx 3 \cdot 10^{13}$ cm^{-3} is described

FIG. 4. The main emission line of a sample with thickness $d = 850 \mu$m in reflection geometry at 2 K and for two pump powers P ($P_{max} \approx 1$ W, $\lambda = 1.06 \mu$m): $P = 0.024 P_{max}$ (solid line) and $P = P_{max}$ (dashed line). The short-wavelength wing of the line was analyzed using the formula (13) with $\delta = 1.1$ meV; T_{e-h} is the value of the parameter T in the formula (3) and was obtained as a result of this analysis: $T_{e-h} = 4.0$ K ($\square$) and 5.6 K (O):

satisfactorily by the formula (2) with $E_g = 234.35$ meV, $E_F = 1.2$ meV, and $T = 2$ K. For a different sample it is necessary to take $E_g = 234.4$ meV and $E_F = 1.4$ meV. In addition, in order to describe satisfactorily the short-wavelength edge of the line, we had to assume that the electron temperature is higher than the lattice temperature and is equal to ≈ 3 K. We note that the low-frequency tail of the long-wavelength wing of the emission lines of both samples (Fig. 2) cannot be described by the expression (2) for any values of the adjustable parameters.

Third, for interband recombination of degenerate electrons and holes, under the condition that the density of nonequilibrium current carriers is higher than that of the free carriers in the unexcited sample, while the lifetime is determined by a different recombination channel and does not depend on the carrier density, the intensity of luminescence characteristically depends quadratically on the level of excitation. As we saw above, such a dependence was observed in both our experiments and other work.[12-15]

Thus in accordance with the results of a number of studies[12-15,18] our experimental data could have been regarded as confirming the overall features of the interpretation, discussed here, of the main emission line. However there are two serious arguments against such an interpretation: 1) the existence of a low-frequency tail that is not described by the expression (2) and 2) the appreciable difference between the value of E_g (lower by $\Delta E \simeq 2.4$ meV), obtained by analyzing the shape of the line according to the formula (2), and the width of the band gap [the present value is $E_g \simeq 236.8$ meV (Ref. 16)]. Moreover, as one can see from Figs. 2 and 4, the main emission line lies practically entirely at energies less than E_g. In addition, if the low-frequency tail can be described phenomenologically by an expression of the type (2), transformed taking into account the tails of the density of states,[18] then the question of the spectral position of the emission line requires a more careful analysis.

We shall examine briefly the possible reasons for the long-wavelength (with respect to E_g) shift of the emission line. This shift could have been due to the polaron effect.[23] The calculations of Benney and Rice[24] give a polaron shift $\Delta E_p \simeq 2.1$ meV in indium antimonide, close to the experimental value $\Delta E \simeq 2.4$ meV. In the case of weakly bound polarons ($\Delta E_p \ll \hbar\omega_{op}$, where $\hbar\omega_{op} = 23.9$ meV is the energy of the longitudinal optical phonon), however, the absorption edge is formed by transitions into polaron states, and for this reason in this case analysis of the absorption spectrum gives the value of E_g taking into account the polaron shift.

Another possible reason could be the renormalization of the width of the band gap due to the decrease of the energy of the interacting particles because of the spatial correlations in the electron-hole plasma.[25] If it is assumed that the main emission line is related with interband transitions, then the electron density in the excited crystal can be determined from the Fermi energy obtained by analyzing the spectra with the help of Eq. (2):

$$n = \frac{(2m_e E_F)^{3/2}}{3\pi^2 \hbar^3}. \tag{3}$$

For a sample with the equilibrium electron density $3 \cdot 10^{13}$ cm^{-3} (the emission spectrum of this sample is the lower spectrum in Fig. 2) an estimate based on this formula gives

$n \approx 2.9 \cdot 10^{14}$ cm^{-3}, while according to existing calculations[24] the observed shift ΔE can be produced by interaction between the carriers only for carrier densities $n > 10^{15}$ cm^{-3}.

Finally, the shift of the emission spectrum into the long-wavelength side could be associated with the presence of tails arising in the density of states of the allowed bands as a result of fluctuations of the concentration of charged impurities. We shall see below that this is exactly what explains the spectral position and shape of the main emission line.

2. Absorption and emission of light with a deficit of the photon energy. First we present the familiar ideas about optical transitions between states belonging to the tails of allowed bands, and we present the corresponding formulas, which we need in order to explain and analyze the experimental data.[23,26] The charge of the impurity atoms, distributed randomly over the volume of a crystal, creates fluctuations of the electrostatic potential, which warps the edge of the allowed bands, so that electronic states (tails of the density of states) appear at energies corresponding to the forbidden band of a pure semiconductor. Gaussian fluctuations of the impurity concentration with a scale of the order of the screening radius r_0 make the main contribution to the potential. The rms potential energy of an electron in the field of such fluctuations (the characteristic depth of the potential wells formed) is equal to

$$\gamma = (2\pi)^{1/2} \frac{e^2}{\varkappa r_0} (N_t r_0^3)^{1/2}, \tag{4}$$

where $N_t = N_D + N_A$ and $\varkappa$ is the permittivity of the crystal. This theory is usually applied to strongly doped semiconductors. We, however, are interested in the large-scale potential under conditions of weak doping ($a_e^3 N_D \ll 1$, $a_h^3 N_A \ll 1$; a_e and a_h are the Bohr radii of the electrons and holes, respectively). In this case, screening at low temperatures occurs owing to the spatial redistribution of the majority charge carriers, bound on atoms of the main impurity, and the screening radius in the case of strong compensation ($1 - K \ll 1$) is given by the formula[26]

$$r_0 = \frac{(1+K)^{1/3}}{(1-K)^{2/3}} N_D^{-1/3} \tag{5}$$

(for an n-type semiconductor).

The main characteristic of the energy spectrum of a semiconductor that reflects the average effect of the fluctuation potential is the density of states $g(\varepsilon)$. In the quasiclassical approximation ($\gamma \gg \hbar^2/m_e r_0^2$, $\gamma \gg \hbar^2/m_h r_0^2$) the density of states in the region of the so-called "Gaussian tail" is described by the expression

$$g(\varepsilon) = g(0) \exp(-\varepsilon^2/2\gamma^2), \tag{6}$$

where the energy ε is measured in a direction into the forbidden band from the boundaries of the unperturbed allowed bands. The tail of the valence band is described by the formula (6) in the energy range

$$0 < \varepsilon < \gamma^{4/3} \left\{ E_A \ln^{-2} \left[\left(\frac{\gamma}{E_A} \right)^2 (N_A a_h^3)^{-1} \right] \right\}^{-1/3}, \tag{7}$$

where E_A is the ionization energy of an isolated acceptor. In the analogous inequality for the conduction band the quantities referring to the acceptors must be replaced by the corresponding parameters of the donors.
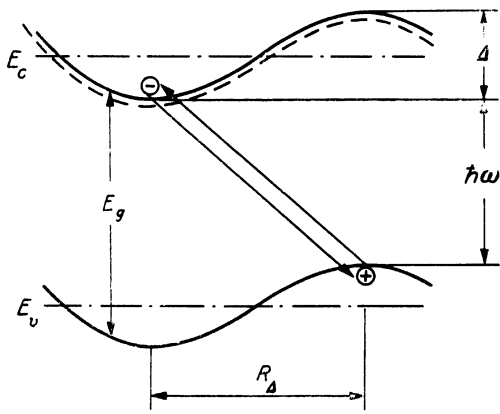
FIG. 5. Diagram of transitions accompanying the absorption and emission of photons with energy deficit Δ: E_c and E_v are the limits of the unperturbed allowed bands (dot-dashed straight lines). The solid lines show the limits of the bands curved by the impurity potential; the dashed line shows the energy levels of the donors.

We shall study the absorption of light when the photon energy is less than the width of the band gap, i.e., when $\Delta \equiv E_g - \hbar\omega > 0$. Such absorption is possible in a nondegenerate semiconductor, when the regions of the crystal in which the electron is located in the initial and final states are spatially separated, i.e., for electron transitions between the hills of the valence band and the valleys of the conduction band, which are formed as a result of the fluctuations of the impurity potential (Fig. 5). The shape of the absorption edge in a strongly doped degenerate semiconductor has been calculated in the quasiclassical approximation for electrons and holes in Refs. 27 and 28 by the method of optimal fluctuation.[26] The absorption coefficient for a photon with energy deficit Δ is proportional to the product of the probability of the appearance of fluctuations of the impurity concentration of scale R, ensuring formation of a barrier of height Δ, and the tunneling probability of carriers over a distance R through the barrier Δ. In the region of high photon energy deficits, where the absorption coefficient $\alpha(\Delta)$ is exponentially small, the product of these probabilities as a function of R has a sharp maximum at

$$R_\Delta = a_{ex}\left(\frac{\Delta}{2E_{ex}}\right)^{3/4}(N_t a_{ex}^3)^{-1/2} \qquad (8)$$

(optimal fluctuation), where E_{ex} is the binding energy and a_{ex} is the Bohr radius of the exciton. In the region where the main contribution to the absorption is determined by the optimal fluctuations, the spectral dependence of the absorption coefficient has the form

$$\ln\frac{\alpha(\Delta)}{\alpha(0)} = -\frac{2}{5\pi^{1/2}}\left(\frac{\Delta}{2E_{ex}}\right)^{5/4}(N_t a_{ex}^3)^{-1/2} = -\left(\frac{\Delta}{\delta}\right)^{5/4}, \qquad (9)$$

where we have introduced the notation

$$\delta \equiv (1250\pi^2)^{1/5}(N_t a_{ex}^3)^{2/5}E_{ex}. \qquad (10)$$

In the derivation of Eq. (9) the screening of the Coulomb potential of the impurities was neglected, and for this reason it is valid if $R_\Delta < r_0$, as a result of which this formula cannot be used for values of Δ that are too large. On the other hand, it is applicable only when the absorption coefficient is exponentially small. These conditions limit the range of ap-

plicability of the expression (9) to the interval

$$2E_{ex}(N_t a_{ex}^3)^{2/5} < \Delta < 2E_{ex}(r_0/a_{ex})^{4/3}(N_t a_{ex}^3)^{2/3} \equiv \Delta_1. \qquad (11)$$

If the size of the optimal cluster is greater than the screening radius ($\Delta > \Delta_1$), then fluctuations of size r_0 make the main contribution to absorption with photon energy deficit Δ, and

$$\ln\frac{\alpha(\Delta)}{\alpha(0)} = -\frac{\Delta^2}{2\gamma^2}, \qquad (12)$$

i.e., the spectral behavior of the absorption coefficient is identical to the energy dependence of the density of states (6).

We now discuss the reverse process—emission of light in the process of recombination of electrons occupying the valleys of the conduction band with holes occupying neighboring hills of the valence band, which are potential wells for the holes (Fig. 5). In contrast to absorption of light, recombination emission is usually observed under substantially nonequilibrium conditions, when excess charge carriers are generated in the semiconductor by means of irradiation or some other method. In strongly doped semiconductors the distribution of holes over localized states of the tail can differ appreciably from the quasiequilibrium distribution (for $m_e \ll m_h$ it is usually assumed that electrons are in quasiequilibrium),[23] and the real filling of the states with nonequilibrium holes must be taken into account when the luminescence intensity is calculated. The luminescence spectrum of a strongly doped compensated semiconductor was calculated in Ref. 29 by the optimal-fluctuation method. The calculations showed that the shape of the short-wavelength edge of the spectral line is described by the formula

$$J(\Delta) \propto \alpha(\Delta)\exp(\Delta/kT), \qquad (13)$$

where $\alpha(\Delta)$ is determined by the expression (9). One can see from Eq. (13) that the rate of decrease of the radiation intensity as ω increases (as $\Delta = E_g - \hbar\omega$ decreases) is determined by the temperature of the sample.

The theory predicts that the shape of the low-frequency wing of the emission line must depend strongly on the pumping level. For very low levels of excitation the probability that states in the tail of the valence band are filled with holes is very low, $q_h \ll 1$, and the shape of the long-wavelength edge of the luminescence line is identical to that of the density of states described by the formula (6). For high pumping intensities all "hole" wells in the tail of the valence band are occupied ($q_h \approx 1$), and

$$J(\Delta) \propto \alpha(\Delta). \qquad (14)$$

Here the absorption coefficient $\alpha(\Delta)$ is determined by the expression (9) with $\Delta < \Delta_1$, where Δ_1 is given by Eq. (11), or the expression (12) for large Δ (at lower frequencies).

3. Analysis of absorption and luminescence spectra and discussion. The result of the analysis of the absorption spectrum (Fig. 1) using the formulas presented in Sec. 2 is shown in Figs. 6 and 7. Two sections can be clearly seen on the curve of $\alpha - \alpha_0$ versus Δ^2 (Fig. 6) ($\alpha_0 = 7.7$ cm^{-1} is the magnitude of the phonon absorption arising as a result of transitions from shallow-acceptor levels into the conduction band[30]). For large photon energy deficits ($\Delta^2 \gtrsim 12$ meV^2) $\log(\alpha - \alpha_0)$ is a linear function of Δ^2, i.e., it varies in accor-
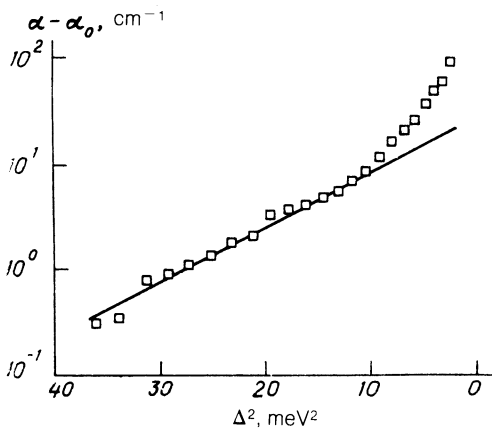
FIG. 6. The difference $\alpha - \alpha_0$ versus Δ^2; $\alpha_0 = 7.7$ cm^{-1} is the absorption coefficient at $\hbar\omega = 230$ meV; $\Delta = E_g - \hbar\omega$ and E_g 236.8 meV; $\square$—are the experimental data taken from Fig. 1.
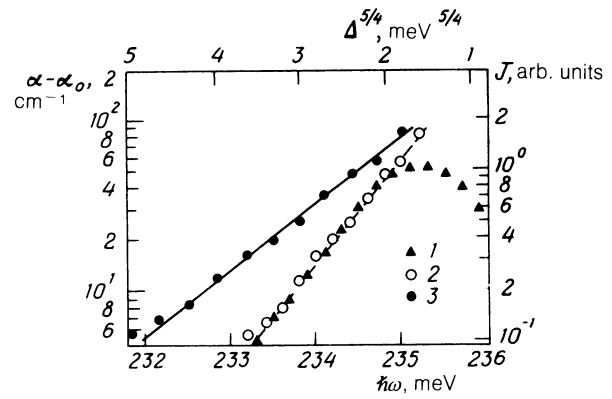

FIG. 7. 1) Luminescence spectrum $J(\hbar\omega)$ and 2, 3) absorption spectrum $\alpha(\hbar\omega) - \alpha_0$. The solid straight line was obtained by analyzing the absorption spectrum 3 using the formula (9) (scale at the top); $\alpha_0 = 7.7$ cm^{-1}.

dance with the formula (12). The slope of this straight line gives the value $\gamma \approx 2$ meV for the rms fluctuation of the impurity potential. For small Δ^2 ($\lesssim 12$ meV^2) the dependence of $\log(\alpha - \alpha_0)$ on Δ (and correspondingly on $\hbar\omega$) is nearly linear (dashed straight line in Fig. 7). In order to compare the observed form of the absorption spectrum for small values of Δ with the form predicted by the expression (9), in Fig. 7 the experimental points are also presented in the coordinates $[\Delta^{5/4}, \log(\alpha - \alpha_0)]$; the slope of the solid line drawn through these points gives the value ≈ 1.1 meV for the parameter δ determined by the formula (10).

We now present some theoretical estimates for a sample with $n \approx 1.2 \cdot 10^{14}$ cm^{-3}, whose absorption spectrum was analyzed above. For this sample we have $K = N_A/N_D \approx 0.43$ and $N_D \approx 2.1 \cdot 10^{14}$ cm^{-3}. Substituting these values (for lack of any better ones) into the formula (5), though this formula is probably not completely applicable for such values of K, we obtain for the screening radius $r_0 \approx 2.8 \cdot 10^{-5}$ cm. Then, with the help of Eq. (4) we find $\gamma \approx 1.8$ meV (with $\varkappa = 17.9$). An estimate of the parameter δ from the formula (10) with $E_{ex} \approx 0.5$ meV and $a_{ex} \approx 6.4 \cdot 10^{-6}$ cm gives $\delta \approx 1.2$ meV. These values of γ and δ are in good agreement with the experimental results.

An estimate of the values of Δ which bound the region of applicability of the formula (9) in accordance with the inequality (11) shows that absorption can be determined by the optimal fluctuations of the impurity concentration in the range $0.4 \lesssim \Delta \lesssim 1.5$ meV. The upper limit of this range is somewhat lower than the experimental value $\Delta_1 \approx 3.2$ meV (Figs. 6 and 7). Finally, estimates of the right-hand side of the inequality (7) with $E_A = 8$ meV and $a_h = 2.3 \cdot 10^{-7}$ cm and of the analogous inequality for electrons shows that the density of states of both allowed bands must have the Gaussian form (6) in the entire energy interval studied ($\Delta_h \lesssim 6$ meV and $\Delta_e \lesssim 10$ meV).

Thus the above theory of interband absorption of light accompanying electronic transitions between the tails of allowed bands[27,28] describes the obtained experimental data well, if the formula (5), which is valid for strongly compensated semiconductors, is employed for the screening radius.

We now analyze the luminescence spectra. The long-wavelength edge of the main luminescence line and the absorption spectrum are compared in Fig. 7. The comparison

shows that in the energy range where the absorption spectrum is described by the expression (9), the frequency dependence of the absorption coefficient is the same as that of the luminescence intensity, in agreement with the relation (14). It should be noted, however, that because the dependence $J(\omega)$ becomes weaker as the maximum of the luminescence line is approached the frequency interval in which $J(\omega)$ is described by the expression (9) is not as wide as the corresponding frequency interval for $\alpha(\omega)$. For this reason the absorption spectrum can be analyzed more accurately than the long-wavelength wing of the emission line.

The results of analysis of the high-frequency wing of the luminescence line with the help of the formula (13) are shown in Fig. 4. In fitting the computed spectrum to the experimental spectrum the parameter δ was set equal to the value 1.1 meV obtained by analyzing the absorption spectrum (Fig. 7) and the fit was made by adjusting the value of T. As one can see from Fig. 4, the formula (13) describes well the short-wavelength wing of the emission line, but the value of the adjustable parameter T giving the best fit between the experimental and computational results is higher than the temperature of the sample, which is equal to 2 K. This means that the system of nonequilibrium charge carriers is overheated relative to the crystal lattice. The increase of the carrier temperature with increasing excitation intensity (Fig. 4) and equilibrium electron density (compare the emission spectra in Fig. 2) is associated with the increase of the efficiency with which energy of the thermalized electrons is transferred to the electron-hole subsystem.[18,31,32] For high levels of excitation the nonequilibrium electrons ($m_e \ll m_h$) occupy not only states in the tail of the conduction band, but also states within the band itself; this is indicated by the appearance of a section on the short-wavelength wing of the emission line that extends to energies higher than E_g (Fig. 4).

In accordance with what we said above in our discussion of the formula (14), the fact that the form of the low-frequency edge of the emission line remains the same in a wide range of pumping intensities (Fig. 4) probably means that $q_h \approx 1$ irrespective of the level of pumping. Moreover, as the concentration of nonequilibrium carriers increases (the pumping level increases) the screening radius should decrease and the potential energy γ should decrease with it, and at the same time the width of the band gap should de-

crease because of the increase in the amount of energy exchanged (the correlation energy in the range of concentrations studied is not significant[33]). For this reason it is surprising that the shape and spectral position of the emission line are constant. It is possible that changes in γ and the exchange energy of the carriers E_{exch} accompanying a change in the level of pumping balance one another.[5] The average change brought about in the width of the band gap by fluctuations of the electrostatic potential and the exchange interaction can be written as

$$\Delta E_g = -\gamma + \tfrac{4}{3} E_{\text{exch}} . \tag{15}$$

For γ the formula (4) with $r_0 = N_t^{1/3}/n^{2/3}$, where n is the electron density in the conduction band, substituted into it can be employed. The last formula is used in the theory of nonlinear screening in strongly compensated semiconductors,[26] and the formula (5) is a consequence of this formula. Then using the standard expression for E_{exch} (Ref. 25) and considering only the electronic contribution to both terms, instead of (15) we obtain

$$\Delta E_g = -\frac{e^2}{\varkappa} \left[(2\pi)^{1/3} \frac{N_t^{2/3}}{n^{1/3}} + 2\left(\frac{3}{\pi}\right)^{1/3} n^{1/3} \right] . \tag{16}$$

The sum in the brackets has a minimum at $n \approx 1.43 N_t$ and near this minimum it changes very little with a quite significant change in n. To what has been said above it should be added that the real situation is much more complicated because of the effect of charge-exchange of impurities accompanying excitation, the nonuniform distribution of the nonequilibrium carriers over the volume of the sample, and other factors.

In concluding our discussion of the luminescence spectra, we shall give an estimate of the parameter δ for a sample with $N_D - N_A \approx 3 \cdot 10^{13}$ cm^{-3}. The emission spectrum of this sample is given by the lower curve in Fig. 2. Analysis of the long-wavelength wing of the emission line using the formulas (14) and (9) gives $\delta \approx 0.82$ meV, while a theoretical estimate using the formula (10) gives $\delta \approx 0.91$ meV, in satisfactory agreement with the experimental results.

Thus the investigation of the shape of the main low-temperature luminescence line of pure n-type indium antimonide, comparison of this shape with the absorption spectrum, as well as theoretical analysis of the luminescence and absorption spectra have shown that this radiation is associated with electronic transitions between spatially separated potential wells for electrons and holes, formed as a result of the warping of the edges of the allowed bands due to fluctuations of the concentration of charged impurities. It should be noted that the smallness of the ionization energy of shallow donors ($E_D \approx 0.5$ meV $< \gamma$) makes it impossible to conclude with confidence from the results of the experiments described above which states the electrons that recombine with holes occupy: in potential wells (valleys) of the conduction band or in donor levels lying beneath these wells. However experiments in a magnetic field showed that the main luminescence line in weak magnetic fields undergoes a diamagnetic shift, which is nonlinear in the intensity of the magnetic field, and the position of the line relative to the energy of an excitonic transition, which also increases with increasing magnetic field strength, remains virtually unchanged. This apparently makes it possible to conclude

that the radiative recombination proceeds through donor levels.

4. Discussion of the spatial distribution of nonequilibrium carriers. We present one other result that follows from the experimental data as a whole: nonequilibrium current carriers fill a volume of the sample with thickness up to 200–300 μm, measured from the excited surface of the sample, and possibly larger.[6] We list the experimental facts. First, the form and intensity of the emission line of a sample with thickness $d \approx 100 \mu$m are virtually independent of the observation geometry. Second, the short-wavelength limits of the luminescence lines of samples of thickness 850 and 550 μm in the case of observation in transmission (Fig. 3) are approximately the same as the limits of the transmission spectra of the samples with thickness 550 and 280 μm (Fig. 1), respectively. Third, the intensity of the luminescence line in the reflection geometry increases as the thickness of the sample decreases, starting with the thickest of the samples studied.

At the present time we do not have a final explanation of this result. We briefly discuss the available possibilities. The diffusion length of nonequilibrium charge carriers in indium antimonide at liquid-helium temperatures is usually estimated to be 1–10 μm.[15,22] The upper limit of this range can be obtained, if the highest measured values of the lifetime $5 \cdot 10^{-7}$ s are used for estimates.[17,18] For this reason, the diffusion mechanism can hardly be responsible for the carrier transport over the observed distances. Among other possible transport mechanisms (expansion of the cloud of degenerate plasma under the action of the internal Fermi pressure,[35,36] entrainment of nonequilibrium carriers by phonon wind[37,38]) the currently preferred mechanism is photostimulated diffusion—generation of electron-hole pairs accompanying reabsorption of the recombination radiation in the sample,[22,39,40] especially since the efficiency of this mechanism increases when the carriers fill the tails of the density of states.[41] Estimates of the distance at which the carriers are found, based on the formulas presented in Ref. 22, are in satisfactory agreement with the experimental results. However further investigations are required in order to obtain a final answer to this question.

CONCLUSIONS

Investigations of the main recombination-radiation line of quite pure samples of n-type indium antimonide, comparison of the form of the long-wavelength wing of this line and the absorption spectrum, and theoretical analysis of the absorption and luminescence spectra have established that the form and spectral position of this luminescence line are determined by large-scale fluctuations of the impurity potential. It was shown that this emission line is related with transitions of electrons, occupying valleys of the conduction band (or shallow donor levels located beneath them), into neighboring hills of the valence band, which are potential wells for holes. The absorption spectrum in the region of the main line and the shape of this line are described well by the theory of optimal fluctuations. In the theoretical analysis of the absorption and luminescence spectra the current value of the width of the band gap $E_g = 236.8$ meV was employed.

It was found that nonequilibrium charge carriers are located at distances of up to 200–300 μm from the excited surface of the sample. These distances are approximately

1145   Sov. Phys. JETP **73** (6), December 1991

Kavetskaya *et al.*   1145

two orders of magnitude greater than the ambipolar diffusion length of carriers. This result has not yet been completely explained and requires further investigations.

We are deeply grateful to L. V. Keldysh, V. D. Kulakovskiĭ, and Al. L. Éfros for a discussion, M. V. Zamkovets for assistance in performing the experiments, and V. S. Ivleva, M. N. Kevorkov, and A. N. Popkov for providing the samples.

---

[1] The idea of a magnetic-field-stabilized EHL was also employed in Refs. 10 and 11 in order to interpret the abrupt shift, observed by the authors, of the induced emission lines of indium antimonide. However the experiments described in these works were performed at a temperature ≈ 5 K, which, as can be judged from the exciton work function of EHL,[6] exceeds the critical temperature even for significantly higher magnetic field strengths than those employed in Refs. 10 and 11.

[2] The preliminary results of these investigations were reported in Ref. 21.

[3] The results obtained in the absence of a magnetic field can also be explained under the assumption that the radiatively recombining electrons occupy not donor levels but rather "valleys" of the conduction band, i.e., recombination is of an interband character. The behavior of the main emission line in a magnetic field, however, apparently makes it possible to draw the conclusion presented in the text.

[4] This result is different from the result obtained in Ref. 9, where a linear dependence of the intensity of luminescence on the pump power was observed. However it agrees with the data of a number of other works.[12–15]

[5] We are grateful to B. L. Gel'mont and V. I. Perel' for making this suggestion.

[6] Close values for the ambipolar diffusion length were obtained in an investigation of the current-voltage characteristics of $p^+ - p - n^+$ structures based on pure p-InSb.[34]

---

[1] C. R. Pidgeon and S. H. Groves in *Proceedings of the 9th International Conference on the Physics of Semiconductors* (Moscow, 1968), Nauka, Leningrad (1969), p. 327.

[2] C. R. Pidgeon and S. H. Groves, Phys. Rev. **186**, 824 (1969).

[3] S. Zwerdling, W. H. Kleiner, and J. P. Theriault, J. Appl. Phys. Suppl. **32**, 2118 (1961).

[4] E. J. Johnson, Phys. Rev. Lett. **19**, 352 (1967).

[5] L. M. Kanskaya, S. I. Kokhanovskiĭ, R. P. Seĭsyan, and Al. L. Éfros, Fiz. Tekh. Poluprovodn. **16**, 2037 (1982) [Sov. Phys. Semicond. **16**(11), 1315 (1982)].

[6] I. V. Kavetskaya, Ya. Ya. Kost', N. N. Sibel'din, and V. A. Tsvetkov, Pis'ma Zh. Eksp. Teor. Fiz. **36**, 254 (1982) [JETP Lett. **36**(7), 311 (1982)].

[7] I. V. Kavetskaya and N. N. Sibel'din, Pis'ma Zh. Eksp. Teor. Fiz. **38**, 67 (1983) [JETP Lett. **38**(2), 76 (1983)].

[8] N. A. Kalugina, *Author's Abstract of Dissertation for Degree of Candidate in Physicomathematical Sciences*, Institute of the Physics of Semiconductors of the Siberian Branch of the USSR Academy of Sciences, Novosibirsk (1986).

[9] R. P. Seĭsyan and Sh. U. Yuldashev, Fiz. Tverd. Tela **30**, 12 (1988) [Sov. Phys. Solid State **30**(1), 6 (1988)].

[10] N. A. Kalugina and E. M. Skok, Pis'ma Zh. Eksp. Teor. Fiz. **38**, 251 (1983) [JETP Lett. **38**(5), 297 (1983)].

[11] N. A. Kalugina and E. M. Skok, Fiz. Tverd. Tela **27**, 528 (1985) [Sov. Phys. Solid State **27**(2), 324 (1985)].

[12] C. Benoit a la Guillaume and P. Lavallard in *Proceedings of the 6th International Conference on Physics of Semiconductors*, Exeter, 1962, Inst. Phys. and Phys. Soc., London (1962), p. 875.

[13] C. Benoit a la Guillaume and P. Lavallard in *Proceedings of the 7th International Conference on Physics of Semiconductors*, Paris, 1964, Dunod Cic., Paris (1965), Vol. 4, p. 53.

[14] J. C. Pehek and H. Levinstein, Phys. Rev. **140**, A576 (1965).

[15] A. Mooradian and H. Y. Fan, Phys. Rev. **148**, 873 (1966).

[16] L. M. Kanskaya, S. I. Kokhanovskiĭ, and R. P. Seisyan, Fiz. Tekh. Poluprovodn. **13**, 2424 (1979) [Sov. Phys. Semicond. **13**(12), 1420 (1979)].

[17] V. I. Ivanov-Omskiĭ, S. I. Kokhanovskiĭ, R. P. Seĭsyan *et al.*, Fiz. Tekh. Poluprovodn. **17**, 532 (1983) [Sov. Phys. Semicond. **17**(3), 334 (1983)].

[18] M. S. Bresler, O. B. Gusev, and A. O. Stepanov, Fiz. Tekh. Poluprovodn. **17**, 1195 (1983) [Sov. Phys. Semicond. **17**(7), 755 (1983)].

[19] M. A. Alekseev, M. S. Bresler, O. B. Gusev *et al.*, Fiz. Tekh. Poluprovodn. **19**, 722 (1985) [Sov. Phys. Semicond. **19**(4), 443 (1985)].

[20] M. S. Bresler, O. B. Gusev, and A. O. Stepanov, Fiz. Tverd. Tela **28**, 1387 (1986) [Sov. Phys. Solid State **28**(5), 781 (1986)].

[21] I. V. Kavetskaya, N. B. Kakhramanov, N. N. Sibel'din, and V. A. Tsvetkov in *Abstracts of Reports at the 6th Colloquium of the Republics on Optics and Spectroscopy of Semiconductors and Dielectrics* (Sukhumi, 1987), Mitsniereba, Tbilisi (1987), p. 7; in *Abstracts of Reports at the 11th All-Union Conference on the Physics of Semiconductors* (Kishinev, 1988), Kishinev, 1988, p. 42.

[22] R. Bichard, P. Lavallard, and C. Benoit a la Guillaume, Solid State Commun. **34**, 467 (1980).

[23] A. P. Levanyuk and V. V. Osipov, Usp. Fiz. Nauk **133**, 487 (1981) [Sov. Phys. Usp. **24**, 187 (1981)].

[24] G. Beni and T. M. Rice, Phys. Rev. B **18**, 768 (1978).

[25] T. M. Rice, in *Solid State Physics*, Vol. 32(ed. H. Ehrenreich, F. Seitz, and D. Turnbull), Academic, New York, 1977, p. 3; T. M. Rice, J. C. Hensel, T. Phillips, and G. A. Thomas, *The Electron-Hole Liquid in Semiconductors* (Russ. Transl. Mir, Moscow, 1980, p. 11).

[26] B. I. Shklovskiĭ and A. L. Éfros, *Electronic Properties of Doped Semiconductors*, Springer-Verlag, New York, 1984.

[27] B. I. Shklovskiĭ and A. L. Éfros, Zh. Eksp. Teor. Fiz. **59**, 1343 (1970) [Sov. Phys. JETP **32**, 733 (1971)].

[28] I. A. Merkulov and V. I. Perel', Fiz. Tekh. Poluprovodn. **7**, 1197 (1973) [Sov. Phys. Semicond. **7**, 803 (1973)].

[29] V. V. Osipov, T. I. Sobolev, and M. G. Foĭgel', Zh. Eksp. Teor. Fiz. **75**, 1044 (1978) [Sov. Phys. JETP **48**, 527 (1978)].

[30] G. R. Allan, H. A. MacKenzie, J. J. Hunter, and B. S. Wherrett, Phys. Status Solidi b **149**, 383 (1988).

[31] V. N. Abakumov, R. N. Lyagushchenko, and I. N. Yassievich, Fiz. Tverd. Tela (Leningrad) **10**, 2920 (1968) [Sov. Phys. Solid State **10**, 2309 (1969)].

[32] M. I. D'yakonov, V. I. Perel', and I. R. Yassievich, Fiz. Tekh. Poluprovodn, **11**, 1364 (1977) [Sov. Phys. Semicond. **11**, 801 (1977)].

[33] P. Lavallard, R. Bichard, and C. Benoit a la Guillaume, Phys. Rev. B **16**, 2804 (1977).

[34] S. P. Grishechkina, Trudy FIAN **89**, 59 (1976).

[35] M. Combescot, Solid State Commun. **30**, 81 (1979).

[36] S. Modesti, A. Frova, T. L. Staehli *et al.*, Phys. Status Solidi **108**, 281 (1981).

[37] V. S. Bazaev, L. V. Keldysh, N. N. Sibel'din, and V. A. Tsvetkov, Zh. Eksp. Teor. Fiz. **70**, 702 (1976) [Sov. Phys. JETP **43**, 362 (1976)].

[38] L. V. Keldysh and N. N. Sibeldin, in *Modern Problems in Condensed Matter Sciences*, Vol. 16 (ed. V. M. Agranovich and A. A. Maradudin), North-Holland, Amsterdam, 1986, p. 455.

[39] W. P. Dumke, Phys. Rev. **105**, 139 (1957).

[40] M. S. Epifanos, E. A. Bobrova, and G. N. Gambkin, Fiz. Tekh. Poluprovodn. **9**, 1529 (1975) [Sov. Phys. Semicond. **9**, 1008 (1975)].

[41] S. G. Dmitriev, Fiz. Tekh. Poluprovodn. **21**, 1503 (1987) [Sov. Phys. Semicond. **21**, 915 (1987)].

Translated by M. E. Alferieff